Genesis of submerged sandstones in Paraná State continental shelf, Southern Brazil, based on cementation patterns, ages and stable isotopes

Bruno Ivan Simioni[1], Rodolfo José Angulo[1], Fernando Alvim Veiga[1], Luiz Henrique Sielski Oliveira[1], Maria Cristina de Souza[1]*

[1] Universidade Federal do Paraná, Laboratório de Estudos Costeiros - Departamento de Geologia
(Av. Cel. Francisco H. dos Santos, 210 - Jardim das Américas - 81530-001 - Curitiba - PR - Brazil)

*Corresponding author: simioni.bruno@outlook.com

ABSTRACT

Beachrocks are a common feature along the Brazilian coast and although their occurrence in intertidal zones is concentrated in tropical regions, similar formations have been described submerged on the continental shelf in subtropical regions. In the state of Paraná, submerged sandstones are present on the continental shelf and their formation could be associated with the cementation of beach sediments. This would provide an excellent indicator of the stabilization of the coastline during lower sea-level periods. In this study, samples were identified and collected in Paraná State, Southern Brazil, at depths between 18 and 33 meters in the continental shelf and at 6 meters depth in the Paranaguá Bay inlet. As *in situ* observations proved problematic, analysis relied mainly on their petrography, mineralogy, ages and isotopic values ($\delta^{13}C$ and $\delta^{18}O$). Whole rock dating demonstrated that the oldest acquired sample was formed 28109-26406 cal. years BP, being exposed to atmospheric conditions during the Last Glacial Maximum. This exposure is reflected in its cements, composed uniquely of microcrystalline and spar calcite, and on its $\delta^{18}O/\delta^{13}C$ values, which indicates formation on a fresh water environment. Contrarily to most carbonate cemented products described along Brazilian coastline, $\delta^{13}C$ values ranged between -26.36 and -51.07‰ on all other samples, interpreted as a result of cement precipitation prompted by methane, either: in a paleo-estuarine/ paleo-lagunar to transgressive environment buried under a pile of coarser material or; after transgression and drowning of organic-rich sediments by coarser sediments, and due to upward migration of methane on the sedimentary column. Both processes would result in cements identified on these samples, apart from the one collected closer to shore which indicates some freshwater influence. Two of the samples separated by 15km distance perpendicularly to the actual coastline and 11m depth difference yielded max and minimum ages of 7913 and 7452 cal. years BP. Such a short time span between these samples could be either the result of their formation on a linked environment or older carbon signature from drowned environments being present on younger cements.

Descriptors: Methane-derived carbonates, beachrocks, submerged sandstones, continental shelf, sea-level indicators.

INTRODUCTION

In coastal environments a series of calcium carbonate cemented products can be found near or submerged in the sea, commonly eoalianites, calcretes (Emery and Cox, 1956; Siesser, 1974), silcretes, cayrocks (Hopley, 1986) and the extensively described beachrocks (*e.g.* Vousdoukas et al., 2007). The latter is widely used as a sea-level indicator, as they may reflect coastline maintenance during some period (*e.g.* Hopley, 1986; Kindler and Bain, 1993; Gischler and Lomando, 1997).

Studies regarding beachrocks from Brazil are mainly focused on Northeastern regions, where beachrocks are commonly found outcropping on intertidal, supratidal and subtidal zones (*e.g.* Branner, 1904; Chaves and Sial, 1998; Manso et al., 2003; Guerra and Sial, 2003; Vieira et al., 2007; Morais et al., 2009) or submerged on continental shelf (*e.g.* Cabral Neto et al., 2010). From Northeastern to Southeastern regions these are also identified outcropping on the intertidal zone (Fúlfaro and Amaral, 1970; Suguio

Submitted on: 23/May/2018
Approved on: 18/September/2018
http://dx.doi.org/10.1590/S1679-87592018019306603

et al., 1985, Mansur et al., 2011) and submerged on the continental shelf (Muehe and Carvalho, 1993).

In Southern regions, beachrocks are described exclusively submerged on the continental shelf. In Parana State, Veiga et al. (2004) described lithified material interpreted as beachrocks occurring at depths between 18 and 31 meters. Similar lithified material is studied in this work. In the state of Santa Catarina, beachrocks fragments were described by Martins et al. (2005) occurring near to palimpsest sediments. In Rio Grande do Sul, an extended submerged parcel called "Parcel do Carpinteiro" was described as a beachrock by Calliari et al. (1994). It is also opportune to mention the occurrence of submerged beachrocks on the continental shelf border between Brazil and Uruguay described by Delaney (1965) and submerged nearshore Bahía Blanca, Argentina (Alliota et al., 2009). In common, all these sandstones occur below latitudes considered ideal for beachrock formation.

The existence of cemented material formed in distinct environments and exposed on a regressive coastline has previously led to the interpretation of other materials as being beachrocks (Russell and McIntire, 1965; Spurgeon et al., 2003). This study aimed to understand the genesis of these rocks and their formation environment, mainly through their petrographic and isotopic characteristics, in order to evaluate if they could be interpreted as true beachrocks (Hopley, 1986) and, therefore, if they could be useful as sea-level indicators.

MATERIALS AND METHODS

Regional settings

The study area (Figure 1) is located on the Southern Brazilian coast, between 25° - 26° S and 49° - 47°55' W. It has a subtropical humid climate, with average rainfall of 2435.8 mm/year and minimum and maximum average temperatures between 16°C - 18°C and 25°C - 27°C, respectively (Vanhoni and Mendonça, 2008).

The adjacent coastal plain is constituted mostly of regressive Holocene and Pleistocene sand deposits, where Angulo (1993; 2004) and Angulo et al. (2008) have described extensive regressive barriers (beach ridges) overlying paleoestuarine deposits. This coastal plain is also characterized by the presence of two estuaries - Paranaguá and Guaratuba, where extensive mangroves develop over clayey silt sand banks (Bigarella, 2001).

Submerged and semi submerged sandy depositional features, interpreted as tidal deltas are also described on the bay mouth areas (Angulo, 1999; 2004).

Sedimentary deposits from the continental shelf have been described as being composed mainly by moderately sorted, very fine to fine sands rich in silt, clay and organic matter. Medium to coarse sands are also described and interpreted as relict sediments (Veiga et al., 2004).

Sampling and analysis

Sandstones from 6 different locations (Figure 1, Table 1), comprising a total of 6 samples, were collected using scuba diving equipment, a sledgehammer and chisel. Side scan sonar imaging was performed on two locations using a DeepVision model DeepEye Sonar System of 340 kHz (DE 340) to further analyze the extension and shape of sandstones. Survey lines were oriented parallel to the isobaths with a lateral range of 50 m and an overlay of 50%. Acquired data were analyzed through the manufacturer's software DeepViewFV. Gain settings were applied, TVG (time variable gain) and AGC (automatic gain control) corrections, and bathy nadir removal (bottom tracking) were done for each sonogram. A manual gain was also applied according to the signal quality.

In general, each sample sized approximately 50 x 20 x 20 cm from which a total of 30 impregnated thin sections were analyzed in conventional petrographic microscope, in order to determine textural features and proportions of matrix, pores, framework grains and cement.

An evenly spaced grid was used for estimating percentages on every square of the grid.

Staining methods described by Warne (1962) and Choquette and Trusell (1978) were used to determine carbonate cements mineralogy of thin sections. Thin sections were partially etched with HCl diluted at 1.5% for 20 seconds prior to staining. Alizarin red-s with HCl diluted at 1.5% and NaOH at 30% was applied and subsequently rinsed with distilled water.

For differentiation between calcite and aragonite, Feigl's Solution (Warne, 1962) was applied and rinsed afterwards. Titan yellow solution (Choquette and Trusell, 1978) was applied for distinction between high-Mg calcite (HMC) and low-Mg (LMC). Thin sections were left to dry overnight prior to microscopic analysis. Mineralogical composition of samples was also determined through x-ray diffractometry performed on

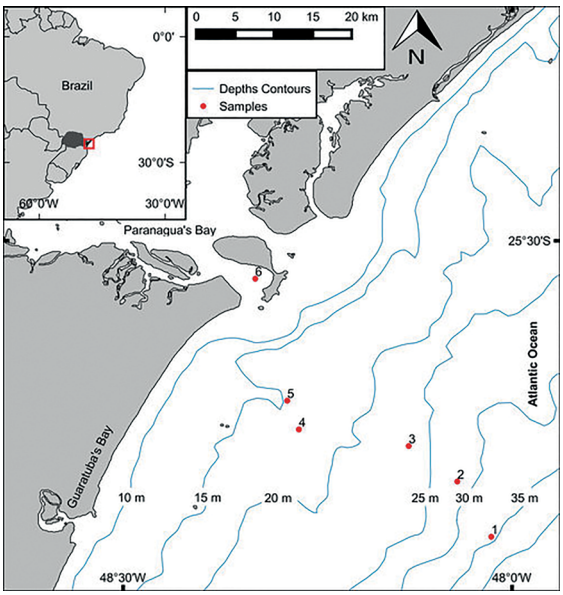

Figure 1. Study area with sample locations and depths contours.

Table 1. Location of samples and its relation to the sea level.

Sample	Latitude (S)	Longitude (W)	Depth (m)
1	25.8810	48.0264	33
2	25.8099	48.0701	29
3	25.7641	48.1325	22
4	25.7427	48.2737	21
5	25.7056	48.2887	18
6	25.5489	48.3303	06

bulk samples which, due to their heterogeneous nature, can have methodological limitations.

Additional petrographic investigations were performed in 30 freshly broken samples using a PHENOM PRO scanning electron microscope (acceleration voltage of 5-10 kV) and a JEOL JSM-6360LV scanning electron microscope (acceleration voltage of 30 kV) supplemented with elemental composition by energy dispersive spectroscopy (EDS) from THERMO NORAN which allows further analysis of cement mineralogy. Cementation patterns were described as referred to by Adams and MacKenzie (1998), Scholle and Ulmer-Scholle (2003) and Flugel (2010).

Conventional radiocarbon dating (^{14}C) was performed on 3 bulk rock samples (approximately 250-300 grams of sample) at *Centro de Energia Nuclear na Agricultura* - CENA (Center for Nuclear Energy and Agriculture) (Piracicaba, São Paulo) and on 1 bioclast sample at Geochron Laboratories (Chelmsford, Massachusetts) with purpose of determining ages. Samples have had incrustrating fauna removed and were dried prior to radiocarbon dating. Radiocarbon ages were calibrated using the program CALIB v. 6.0 (Reimer et al., 2009; Stuiver et al., 2009) and were corrected to a ΔR of 8±17 years as defined in Angulo et al. (2005) for southern Brazil.

Stable isotope analysis ($\delta^{13}C$ e $\delta^{18}O$) were performed at *Núcleo de Estudos Geoquímicos - Laboratório de Isótopos Estáveis* (NEG-LABISE) at Federal University of Pernambuco. No cements were isolated, but after micro-petrographic analysis 12 samples were selected based on the cement prevalence. Of these, 11 correspond to bulk rock samples (approximately 10-20 grams of sample) where bioclasts were mechanically removed using chisel and hammer. Circa of 20 mg of material was powdered using a hand drill and samples were reacted with 100% orthophosphoric acid. The CO_2 released from the reaction was analyzed in a dual inlet, triple collector mass spectrometer (VG-ISOTECH SIRA II), using the BSC (Borborema skarn calcite) reference gas, calibrated against NBS-18, NBS-19 and NBS-20.

RESULTS

Sandstones occurrence and lithology

Studied sandstones were found and collected on the inner shelf, at depths ranging from 18 to 33 meters, 17 to 48 kilometers from the present shoreline and on the Paranaguá Bay inlet, submerged at 6 meters depth (Figure 1). Those present at the inner shelf occur adjacently to areas where relict sediments have been described (Veiga et al., 2004; 2006).

They occur as broken and displaced slabs not longer than 3 meters, partially buried by sand.

Their elevation relative to the seafloor is not higher than 1 meter. Beddings or depositional features cannot be observed *in situ* due to incrustation and weathering. Sometimes slabs can spread up to 60 meters long on the seafloor (Figure 2).

The sandstones are generally massif, and only incipient stratification can be observed on samples, although some distinctive characteristics could be observed on 3 samples: On sample 1, it was possible to determine that most of its bioclasts are composed of bryozoans.

Also, feldspars constitute 10% of framework grains on this sample (Figure 3a). Sample 4 has two separate cemented layers, indicating distinctive cementation

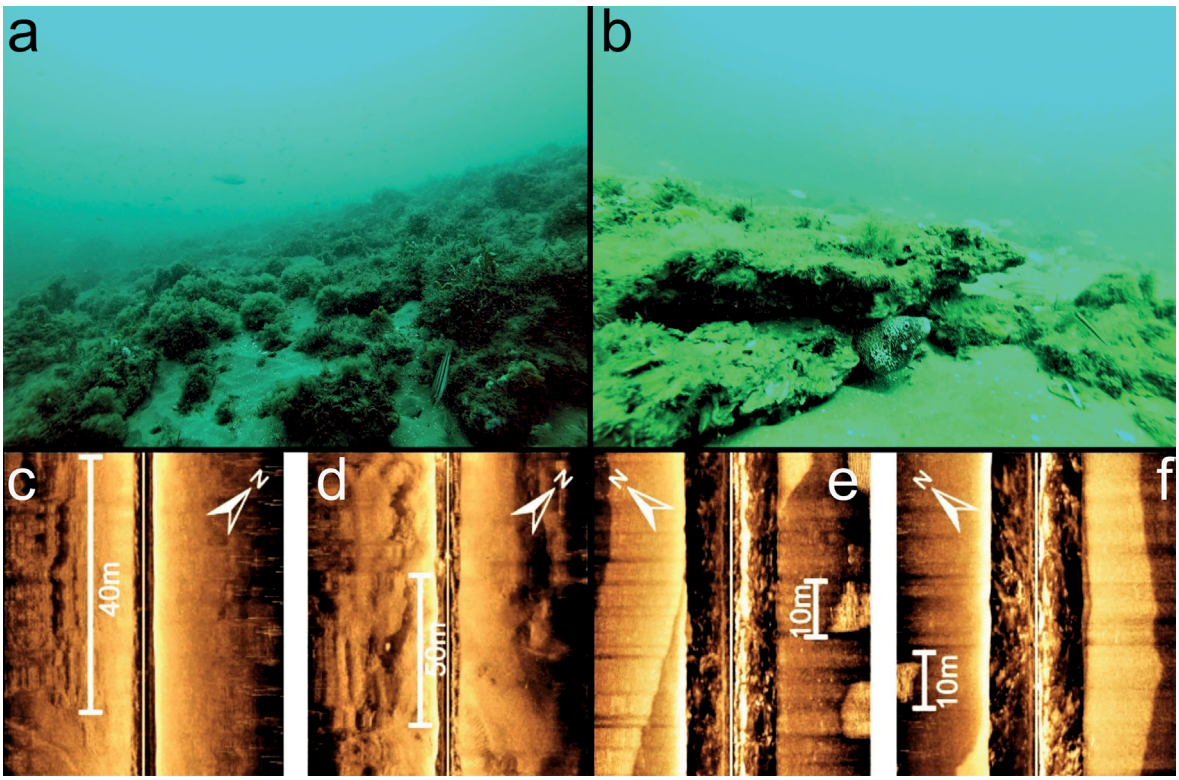

Figure 2. (a,b) Pictures of sandstones at the site where sample 3 was collected. In general all studied sandstones have similar characteristics and distribution (Photo: Marcelo Soeth, Fish Ecology Laboratory - UFPR). Side Scan Sonar images of sandstones (measurement bar indicating main sandstone body) where samples 6 (c,d) and 5(e,f) have been collected.

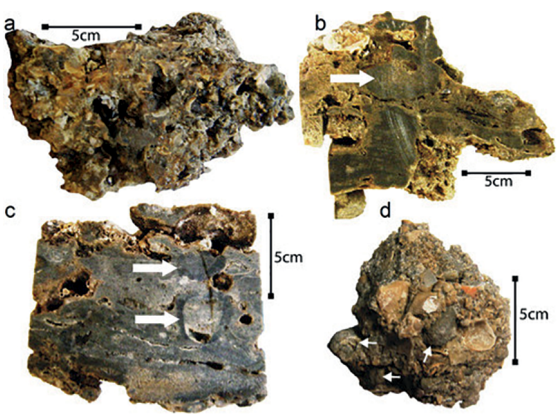

Figure 3. Samples cut in half (a-c); (a) sample 1; (b) sample 4, white arrow indicates incorporated intraclasts. (c) Sample 5, white arrow points to biogenic structure interpreted as a tube section corresponding to *Ophiomorpha nodosa*; (d) top view from shells and rounded intraclasts (white arrows) on sample 4.

processes. The first layer is composed by intraclasts up to 20 cm, exhibiting rounded edges and physical dissolution or abrasion characteristics. Bioclasts are rarely observed and it is composed predominantly of very fine sand. These have been incorporated into the second layer which is predominantly composed of bioclasts, first stage's well-rounded intraclasts and coarse sand quartz grains (Figure 3b and 3d). Sample 5although massif, shows tubes similar to *Ophiomorpha nodosa* (Figure 3c).

Sandstones are constituted mainly by fine to coarse, poorly to moderately sorted, subangular to well-rounded sand, composed of mainly quartz grains and secondarily by bioclasts (fragments of bivalve, echinoids, gastropods, bryozoan - average 8.3%), usually greater than 2 mm and less than 5 cm (Table 2). To a lesser amount: feldspars (average 4.1%), unclassified heavy minerals (average 2.3%) and intraclasts that are pre-cemented fragments incorporated to the sandstones (average 2.6%). Average amounts of framework, cement and porosity are, respectively: 63.3%, 29.4% and 7.3%. These sandstones can be classified as hybrid arenites (Pettijohn et al., 1987; Stow, 2005).

Cements Diagenetic features and mineralogy

a) Fibrous and acicular prismatic aragonite was the most common cement type found on the studied samples. Differentiation between fibrous and acicular aragonite was only possible through SEM images (Figure 4b, 4c)

Table 2. Percentage of framework grains, cements and porosity for studied sandstones.

Sample	1 (%)	2 (%)	3 (%)	4 (%)	5 (%)	6 (%)	Average (%)
Mono. quartz	29	40.5	35.5	24.8	40.2	41.2	35.2
Polyc. quartz	7	13	14.5	9	10.6	11.6	11
Feldspar	10	3	2	2.8	3.5	3.3	4.1
Fragments	6	1	2	1	1.8	1.8	2.3
Bioclasts	18	5	6	7	7.3	6.3	8.3
Cement	20	32.5	33	31	29.3	30.8	29.4
Porosity	10	5	7	10	7	4.8	7.3
Intraclasts	0	0	0	14.5	0.5	0.5	2.6

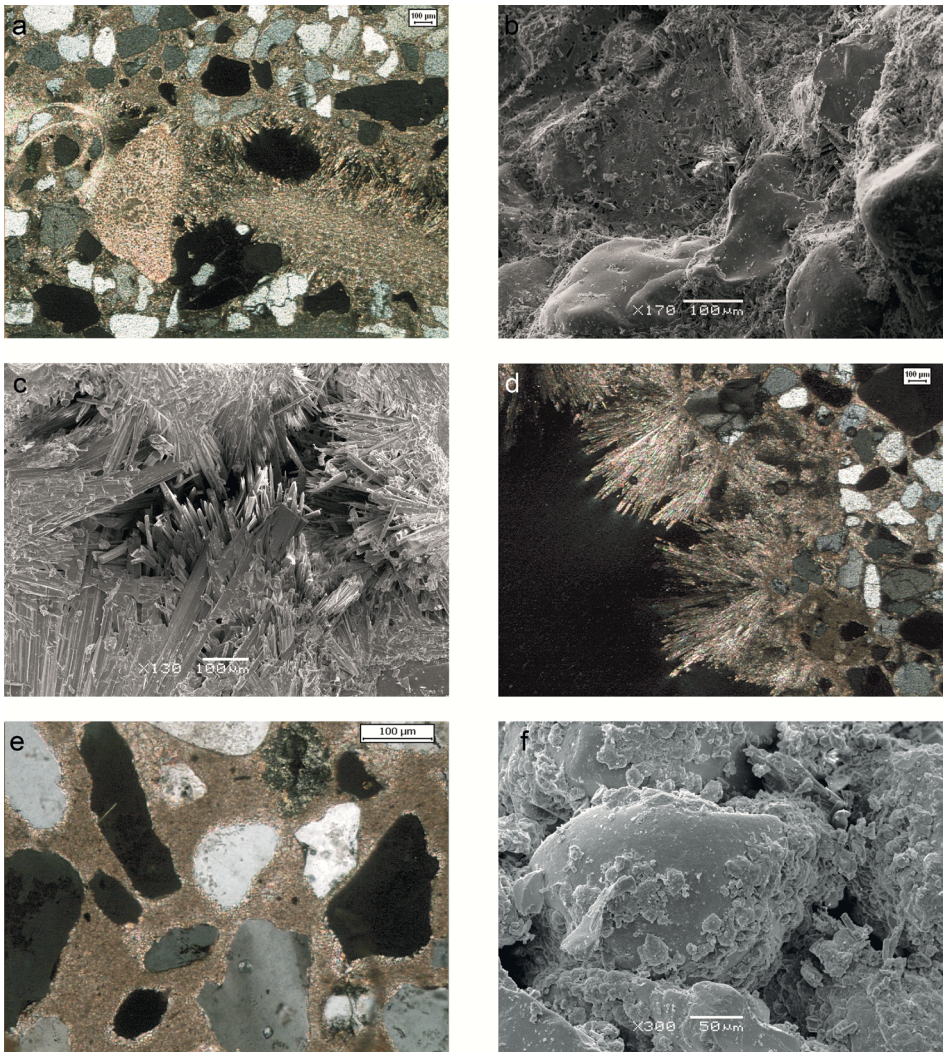

Figure 4. (a) Tight mesh of acicular and fibrous aragonite filling intergranular and pore spaces, aragonite projecting to pore interiors from grains and bioclasts; //P. (b) SEM image of same sample, detail of tight meshes. (c) SEM image of fibrous and acicular crystals projecting to pore interior. (d) Splays and botryoids on secondary porosity; //P. (e) Crypto to microcrystalline HMC cement filling intergranular space; //P. (f) SEM image of same sample, showing aggregates of crypto to microcrystalline cements.

since these two cement types formed a tight mesh, undistinguishable in common petrographic microscope (Figure 4a). Thus, for statistical purposes, both types were grouped. Fibrous crystals normally present a blunt termination, hexagonal shape, length up to 500 µm and width higher than 10 µm, maximum 20 µm.

Acicular crystals present a needle-like crystal, with acute termination, length up to 400 µm and width between 2 - 15 µm. These cements commonly grow from the surface of the grain separated by a high-Mg crypto to microcrystalline coating except when growing from bioclasts surfaces.

Both cements fill intergranular and pore spaces, most commonly forming tightly encompassed lathlike meshes. Also, fibrous and acicular cements were observed projecting into pore interiors, perpendicularly or sub-perpendicularly in relation to their origin, sometimes forming fan-like structures (splays and botryoids) (Figure 4d) more commonly on secondary pores. Fibrous crystals elongate and widen to form rhombic to blunt hexagonal terminations (Figure 4c).

On the presence of bioclasts, these cements tend to form irregularly sized fringes (up to 200 µm long) lining bioclasts grains directly from the grain surface or sometimes filling intergranular space, growing preferably from bioclast to intergranular/pore space. Such fringes were also observed lining pores and siliciclastic grains, although in these cases, they present no more than 50µm long and are separated from the grains by a high-Mg crypto to microcrystalline coating. Eventually, pore-lining fringes can fill the whole pore space forming polygonal contacts. These are the most common cements found on samples 2, 3 and 4 (minimum of 35%, maximum of 60% for all samples - Table 3).

b) The second most common cement is crypto to microcrystalline composed of high magnesium calcite. When observed on petrographic microscope they present brownish to crystalline color (Figure 4e). On SEM image crystals sized less than 5µm, anhedral to euhedral (rhombic) could be observed (Figures 5a and 5b). Silt-sized siliciclastic grains can sometimes be observed (Figure 5a). These cements form coatings or cuticles around framework grains or completely fill intergranular space (Figures 4e and 4f).

These cements usually precede other diagenetic features (fibrous and aciculars), indicating a first incipient cementation. Coatings have variable thickness, covering both carbonate and siliciclastic grains. This cement type constitutes a maximum of 42.5% on sample 5, where it is the main cement, and minimum of 7.5% on sample 4 (Table 3).

c) Fibrous high-Mg calcite in a common petrographic microscope these cements would appear the same as fibrous and acicular aragonite cements, but mineralogy was determined as high-Mg Calcite through staining methods and x-ray diffractometry. This cement type was observed more accurately using SEM, showing elongated hexagonal prismatic cements with up to 200µm long and more than 10µm width and flat termination, looking similar to a column. These cements occur filling intergranular space and pores. They typically overlay each other forming disordered tight meshes or lathlike structures and, eventually, polygonal contacts. Cements are commonly separated from the framework grains by a crypto to microcrystalline coating (Figure 5c). These cement type and fabrics were observed on samples 3, 4 and 5. Percentages are minimum 15% on sample 5 and maximum 26.8% on sample 3 (Table 3).

Table 3. Percentage of cement types on the studied sandstones.

Cement sample	1 (%)	2 (%)	3 (%)	4 (%)	5 (%)	6 (%)
Blocky calcite	69.0	0.0	0.0	0.0	0.0	0.0
Microcrystalline Calcite	26.0	0.0	0.0	0.0	0.0	0.0
Dogtooth Calcite	5.0	0.0	0.0	0.0	0.0	0.0
Fibrous/ Acicular Aragonite	0.0	60.0	48.3	40.0	35.0	0.0
Microcrystalline High-Mg	0.0	40.0	25.0	7.5	42.5	0.0
Fibrous High-Mg Calcite	0.0	0.0	26.8	21.3	15.0	0.0
Granular High-Mg Calcite	0.0	0.0	0.0	25.0	0.0	0.0
Infiltrating Micrite	0.0	0.0	0.0	6.3	7.5	0.0
Granular Low-Mg Calcite	0.0	0.0	0.0	0.0	0.0	100.0

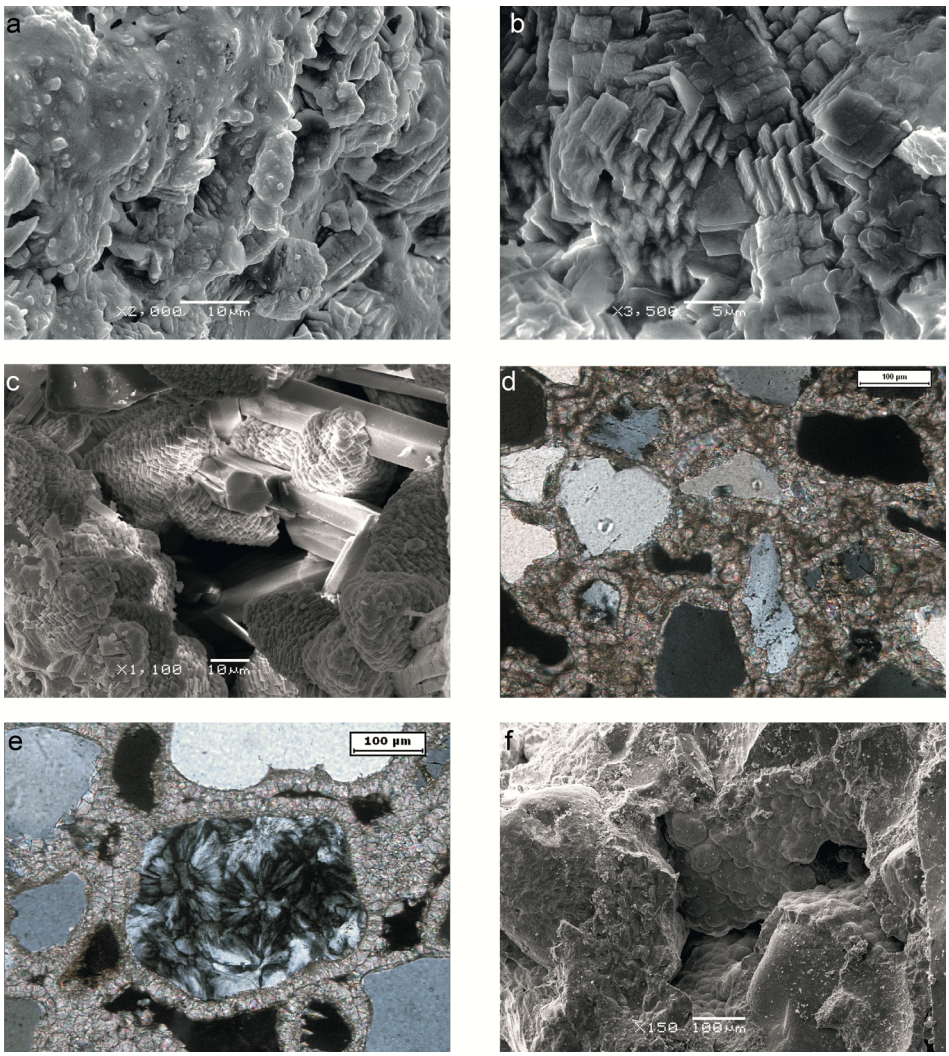

Figure 5. (a) SEM image of anhedral cryptocrystalline cement, note clay sized particles. (b) SEM image, sub-euhedral to euhedral crypto to microcrystalline cements. (c) SEM image, Fibrous HMC growing from euhedral crypto to microcrystalline cements. (d) Granular HMC cements filling intergranular space and forming rims lining grains; //P. (e) Granular Low Mg Calcite, filling intergranular space and lining siliciclastic grains; //P. (f) SEM image, same sample of granular Low Mg Calcite.

d) Granular cements, sized no more than 20µm, are composed of high magnesium calcite.

Examined on SEM, crystals have anhedral to sub-euhedral rhombic form. These are filling intergranular spaces forming a granular mosaic or relatively isopachous rims lining pores and grains (circumgranular), separated from grains surface by a darkish HMC cryptocrystalline cuticle (Figure 5d). This cement was observed exclusively on incorporated intraclasts on sample 4 (Table 3).

e) Granular cements, sized up to 20 µm, are composed exclusively of low magnesium calcite, were observed exclusively on sample 6 and are the only type on this sample. SEM images reveal sub-euhedral to euhedral rhombic crystals (Figure 6a), that when grouped form "framboidal" or "bunch of grapes" structures (Figure 5f). These cements filling intergranular and pore spaces as a granular mosaic, and also forming isopachous rims lining pores and grains (Figure 5e) (Table 3).

f) Blocky calcite cements are composed exclusively of calcite, as confirmed through staining, EDS and x-ray diffractometry. They occur filling intergranular and pore spaces and occasionally bioclasts interior after their partial dissolution, with clear crystals limits. Close to framework grains and bioclasts develop equidimensional crystals

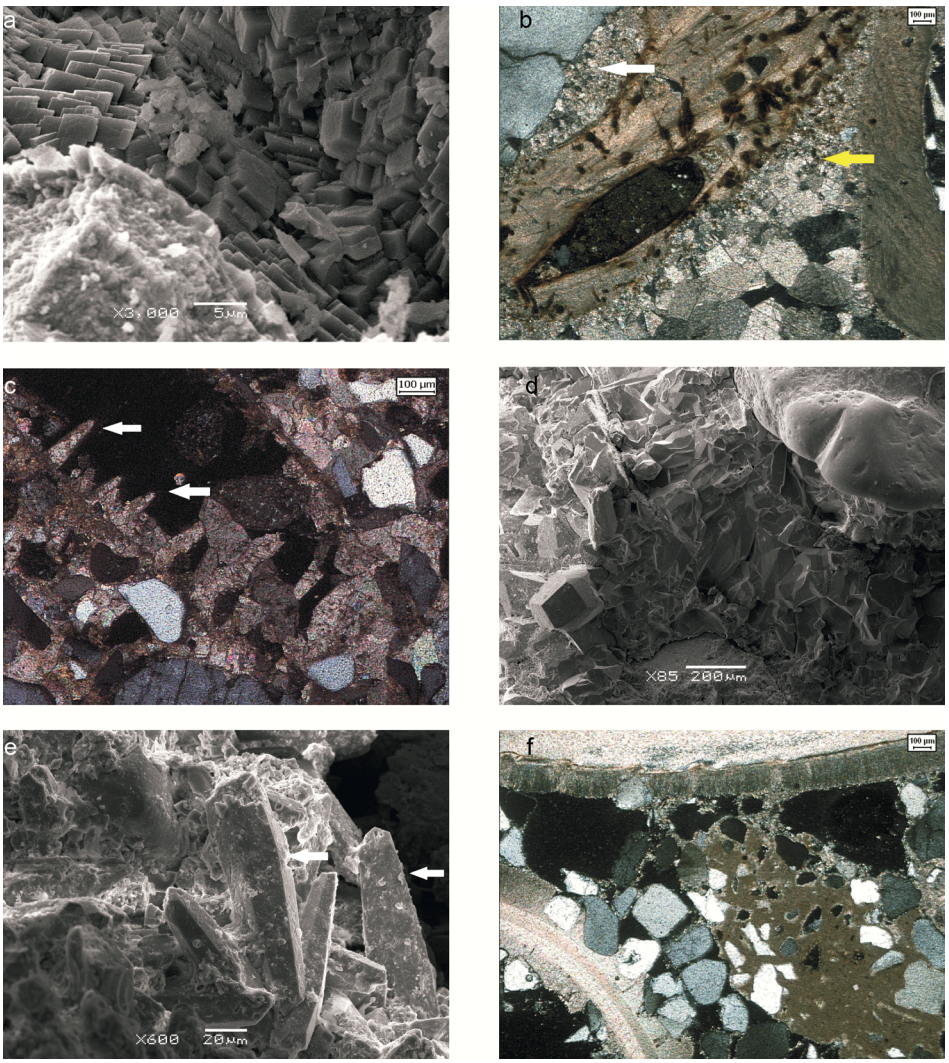

Figure 6. SEM image, sub-euhedral to euhedral rhombic Low-Mg Calcite cements. (b) Microcrystalline (top arrow) and blocky drusy mosaics of calcite (lower arrow, note the cement size increasing towards the center); //P. (c) Dogtooth or bladed calcite projecting to pore interior (arrows). (d) SEM image, same sample as of b showing drusy calcite. (e) SEM image, same sample as of c showing scalenohedral crystals (arrows) projecting from microcrystalline cements.(f) Infiltrated micrite and aragonite rims around bioclasts; //P.

(height/ width 1.3:1) averaging 10 µm, which increase towards the center of pore (drusy mosaics), reaching sizes above 200µm (Figure 6b and 6d). These cements were only observed in sample 1, representing 69% (Table 3).

g) Microcrystalline calcite occurs mainly filling intergranular and pore spaces, sometimes forming a thin crust around siliciclastic grains and bioclasts, preceding blocky calcite (Figure6b). Partial dissolution and recrystallization by microcrystalline calcite was rarely observed. Crystals are anhedral and sized less than 5µm. These cements are observed only on sample 1, representing 26% of its cements (Table 3).

h) Dogtooth (Flugel, 2010) or bladed (Scholle and Ulmer-Scholle, 2003) calcite cements, projecting sub-perpendicularly and perpendicularly to pore interiors as prismatic scalenohedral crystals of at least 50µm and up to 300µm long (Figures 6c and 6e), with height width relation of 2.5:1 and 3:1. These cements are usually separated from framework grains by microcrystalline calcite. Exclusively observed on sample 1, where represents 5% of the sample's cements (Table 3).

The infiltrated micrite consists of micrite masses, with anhedral crystals sized less than 2µm and a great number of foraminifers, diatoms, radiolarians and siliciclastic grains. It was identified on samples 4 and 5, where it occurs filling

voids and intergranular spaces, sometimes forming thin crusts around grains (Figure 6f). Percentages of minimum 6.3% and maximum of 7.5% (Table 3).

Ages, carbon and oxygen isotopic data

Sample dating results ranged from Late Pleistocene to Holocene. Apart from sample 6 on which a bioclast was dated and represents maximum deposition age, all the rest correspond to bulk rock ages, which correspond to a mixed age of framework and cements ages. With the exception of sample 1, with isotopic values $\delta^{13}C$ between -1.18 and -2.11‰, all samples showed highly negative $\delta^{13}C$ values, between -26.36 and -51.07‰. $\delta^{18}O$ isotopic values have ranged from -4.75 and 1.59‰ (Table 4). There are differences of $\delta^{13}C$ values obtained during radiocarbon dating and isotope analysis on samples 2 and 5. This is a result of using the bulk rock for dating whereas for isotope analysis, sandstone fragments with pre-determined cement prevalence were used.

DISCUSSION

Ages

Radiocarbon ages from the dated samples ranges between late Pleistocene and Holocene.

Sample 1 ^{14}C dating resulted in 28109-26406 cal. years BP which correspond, according to Milliman and Emery (1968), to an epoch of low sea-level after the Eemian interglacial period corresponding to Marine Isotope Stage 5e. Analysis of its cement mineralogy and $\delta^{18}O$ isotopes indicates it was formed on a freshwater or meteoric influenced environment, suggesting that approximately 28109-26406 cal. years BP the sea-level was below 33 m than present one. It was not possible to determine if the sandstone formation occur on a foreshore environment, closer to the sea or further inland. Also, little weight should be given to determination of the sandstones exact age as it comprises composed carbon from shells, cements and possibly new foreign carbon when exposed to atmospheric conditions.

Ages from samples 2 and 5 ranged from 7913 to 7452 cal. years BP, corresponding to the transgressive period after the Last Glacial Maximum that occurred approximately 17.000 years BP. These ages have a small timespan considering sample 2 and 5 are over 15km distance from each other and occur at 11m depth difference. Two possible reasons for such contemporaneity are plausible: Firstly that lithification process occurred on a linked environment, such as estuaries, deltas, marshes and mangroves, prompted by the methane oxidation after organic matter burial. As a reference, the actual distance between Paranaguá Bay inlet and its innermost part is *circa* 45 km. Secondly, after the transgression and drowning of Pleistocene organic-rich deposits, methane escape through sedimentary column has been responsible for the formation of these sandstones in a submerged environment.

Table 4. Isotopes and ages results.

Sample	N	^{14}C y BP	^{14}C cal y BP	$\delta^{13}C$.dat (‰)	$\delta^{13}C_{VPBD}$ (‰)	$\delta^{18}O_{VPBD}$ (‰)	D (m)	Lab
1	BR	25450-24750	28109-26406	-1.1	-2.11‰	-4.75‰	33	CENA#533/ MRE
1	BR	-	-	-	-1.18‰	-4.07‰	33	33M
2	BR	8850-8670	7909-7452	-47	-32.64‰	-2.01‰	29	CENA#531/
3	HMC	-	-	-	-46.19‰	-1.33‰	22	22A
3	AR	-	-	-	-47.55‰	0.32‰	22	22B
4	HMC^{+}	-	-	-	-46.54‰	0.23‰	21	21A
4	AR/HMC	-	-	-	-45.11‰	1.59‰	21	21B
4	B	-	-	-	-26.36‰	0.16‰	21	21C
5	BR	8860-8680	7913-7465	-43.47	-50.30‰	0.02‰	18	CENA#259/
6	B	6660-6280	5557-4748	-37.8	-37.93‰	-0.73‰	6	GX-33475/
6	LMC	-	-	-	-36.50‰	1.59‰	6	B2TC

Notes: (N) Sample nature where; HMC - Predominance of High Mg Calcite, AR - Predominance of Aragonite, HMC+ - Granular High Mg Calcite from intraclasts, LMC - Low Mg Calcite, B- Calcareous Bioclast; BR - Bulk rock; (14C y BP) radiocarbon years before present; (14C Cal y BP) radiocarbon calibrated years before present; (δ13C.dat) δ13C obtained from 14C dating; (D) Depth of sample; (Lab) laboratory reference.

Friedman et al. (1971) describe the occurrence of sandstones on United States continental shelf over a drowned floodplain at 79 m depth. Isotopic and dating analysis from cements and shells indicate that the shells that compose such sandstones are younger than the cements.

According to the authors, the methane responsible for cement precipitation has led the older carbon signature to be present on the cements. It is reasonable to conclude that since these cements have precipitated due to methane migration on the sedimentary column their age would correspond to the age of the organic matter deposit. According to Bigarella (2001) actual transgressive-regressive Holocene deposits overly paleo-lagunar deposits rich in organic matter and fine sediments.

Sandstone corresponding to sample 6 occur at 6 m depth in an adjacent area to the Paranaguá Bay inlet, yielding ages of 5557-4748 cal. years BP when mean-sea-level would be at least 1 meter above present sea-level (Angulo et al., 2006). As LMC cements that occur as circumgranular and granular mosaic cements are indicators of precipitation on a meteoric phreatic environment it is very likely that this sample was lithified under such influence, by a process prompted by similar organic matter decay that is suggested for other samples.

Interestingly, not only $\delta^{13}C$ isotopes for the whole sample but also dated bioclast presented highly negative $\delta^{13}C$ values (-37.8 ‰).

Sandstones occurrence

Beachrocks are described on intertidal zones of many beaches along the Brazilian coastline. From Southern São Paulo's Coast towards South, where conditions for beachrock formation are less favorable (Vousdoukas et al., 2007; 2009), similar features to beachrocks are only described on submerged areas (Martins et al., 2005; Calliari et al., 1994). Studied sandstones have been found at depths between 6 and 33 m, which could fill a gap for sea-level history on Paraná's State continental shelf. Due to their characteristics and occurrence in the marine environment, these sandstones resemble beachrocks and are very likely to be interpreted as such. Accordingly to Hopley (1986), the use of beachrocks as a sea-level indicator must be held carefully: primarily, it should be necessary to obtain evidence that the studied object is "true beachrock" *i.e. "*cemented sediments in an intertidal environment of an exposed beach, and not later under a pile of unconsolidated sediments". The author also mentions that the nomenclature "beachrock" should only be used in the case of cementation on typical beaches and not on environments where freshwater is predominant. Also, questions such as: exact position in relation to the exposed beach where cementation took place; state of preservation of studied beachrocks and their depositional structures; fragmentation and destruction by physic-chemical process and re-cementation processes; should be raised when using beachrocks as sea-level indicators (Schroeder, 1979; Kelletat, 2006; Knight, 2007; Kelletat, 2007).

Samples of the inner-shelf (1 to 5) were found on submerged areas, on the vicinity of where fine to coarse, moderately to well-sorted palimpsest sands are described by Veiga et al. (2004; 2006). In general, grains of studied sandstones do not differ greatly from the sediments of the seabed where they sit. If the sandstones diagenesis happened contemporaneously to its deposition, they would have been subject to extensive weathering during Late Pleistocene transgressions and, as observed by Rey et al. (2004), the exposure of a sandstone body on a high energy transgressive environment could change its characteristics and shape significantly. Seabed sedimentary characteristics could also indicate that these sandstones are subject to exhumation by the action of currents and waves. Due to the weathered state of such rocks and as these are subject to incrustation, impairing in *situ* observations, one has to rely on hand samples acquired, disregarding lateral and horizontal continuity. On 18 m depth (sample 5) bioturbation structures were observed corresponding to *Ophiomorpha nodosa*, commonly associated with intertidal and sub-tidal crustaceous (Suguio et al., 1984). In Southern Brazil, *Callichirus major* is the main species related to such structures, producing vertical funnels with usually 2 m and up to 4 m length and which are commonly used as low-tide, intertidal and shallow marine environment indicators (Suguio et al., 1984; Angulo and Souza, 2014). Thus it is possible to infer that the lithified strata correspond to this shallow marine deposit.

Oxygen and Carbon isotopic data

Isotopic and petrographic analyses of sandstones are key tools for determining the processes which triggered cementation (*e.g.* Spurgeon et al*.,* 2003; Vieira and DeRos, 2006).

The results obtained on the present study have been plotted on a graph with $\delta^{13}C$ x $\delta^{18}O$ isotopic data from this work along with other relevant studies, presented in

Figure 7. With the exception of sample 1, all samples presented highly negative $\delta^{13}C$ isotopic values, varying between -26.36‰ and -51.07‰. Accordingly to Moore (1989) organic carbon can exhibit negative $\delta^{13}C$ values (around -24‰) in comparison to marine carbonates (0 to 4‰), whilst extreme negative values (up to -80‰) would be the result of methane oxidation and subsequent cementation. The oxidation of residual organic matter and subsequent cementation would result in cements with positive $\delta^{13}C$ values (Moore, 1989).

Highly negative $\delta^{13}C$ values have been described: on cemented material of fresh/salt water transitional environments where organic matter deposits lies underneath a thin deposit (Roberts and Whelan, 1975; Nelson and Lawrence, 1984), on pockmarks in shallow and deep waters (Hovland et al., 1987) and also on hydrothermal vents and cold seeps (Han et al., 2008).

Nelson and Lawrence (1984) describe the occurrence of carbonate-cemented terrigenous nodes and slabs formed within the water-sediment interface, with $\delta^{13}C$ values between -7‰ and -59‰ on the Fraser River Delta, Canada. According to the authors, cement precipitation was triggered due to degradation of organic matter which was deposited under a thin layer of deltaic sediments. Biogenic methane production, its migration to the surface, and anaerobic/aerobic bacterial fermentation was the proposed process for such origin.

Through similar processes and products, Roberts and Whelan (1975) described the formation of well-cemented crusts on beaches and barriers of the Mississippi River Delta, USA with $\delta^{13}C$ values ranging between -14‰ and -40‰, where Holocene sands transgressed over highly organic marsh deposits. This process is also identified by Friedman et al. (1971) as responsible for submarine lithification at the continental shelf off of Delaware, North America, after transgression over tidal marshes, which would be a common mechanism for promoting marine lithification. Values of $\delta^{13}C$ on these lithified crusts ranged between -8.4‰ for molluscan shells and -44.8‰ for aragonite cements (Friedman et al., 1971). Carbonate cements originated from all above mentioned processes do not differ to those described on true beachrocks in relation to form and mineralogy.

The diagenetic environment from such origin could start on an anoxic environment, well below the sediment surface, as methane oxidation by sulfate-reducing and methanotrophic bacteria occurs. In the case of pockmarks, Hovland et al. (1987) noted that diagenesis on the anoxic (sulfate-reducing) zone would produce some clear characteristics as microcrystalline HMC and the presence of pyrite. As methane that survived this zone migrates upwards and reaches oxic-anoxic and sediment-water boundaries, aerobic oxidation of methane will take place and bicarbonate is produced increasing interstitial waters alkalinity, therefore producing cements common to marine environments (Hovland et al., 1987; Bahr et al., 2007).

Environments rich on shallow biogenic methane comprise areas where organic matter accumulates rapidly, such as fluvial floodplains, estuaries, bays and deltas (Judd and Hovland, 1992). On environments and paleoenvironments rich in organic matter, great methane accumulations can occur, producing gas that either gets trapped on the sediment layers or escape to the water (Burdige, 2006).

344 km north from the study area, Felix and Mahiques (2013) have identified shallow gas formations both on Holocene sediments, which are currently under formation process, and on buried Pleistocene fluvial floodplains. Pockmarks and gas seeps have also been identified in their study, the latter occurring when the sedimentary package is less cohesive, i.e. with coarser sediments. The occurrence of shallow gas generated through methanogenic bacteria on Holocene and pre-Holocene deposits has also been described occurring in enclosed and semi-enclosed areas of southeast (Benites et al., 2015) and southern (Klein et al., 2016) Brazil.

$\delta^{18}O$ isotopes on carbonates normally reflect temperature and isotopic composition of the fluid from which they precipitate, thus fresh water carbonates possess negative $\delta^{18}O$ values whilst marine cements positive values (Moore, 1989). Cements formed within sediment subsurface are also subject to negative $\delta^{18}O$ values (Hovland et al., 1987; Moore, 1989).

Oxygen isotopes on samples from sample 1 have remained between -4.07 e -4.75‰ and their $\delta^{13}C$ between -1.18 e -2.11‰. Such values are normally correlated to cement precipitated under meteoric or mixed marine/meteoric environment (Moore, 1989). Similar values were obtained by Calvet et al. (2003) on Canary Islands' aragonite cements and Guerra et al. (2004) in Northeast Brazil neomorphic aragonite cements, both being interpreted as marine cements under the meteoric/phreatic influence. Also, Spurgeon et al. (2003) have found similar results on LMC bladed spars from a sandstone formed on the meteoric-phreatic environment

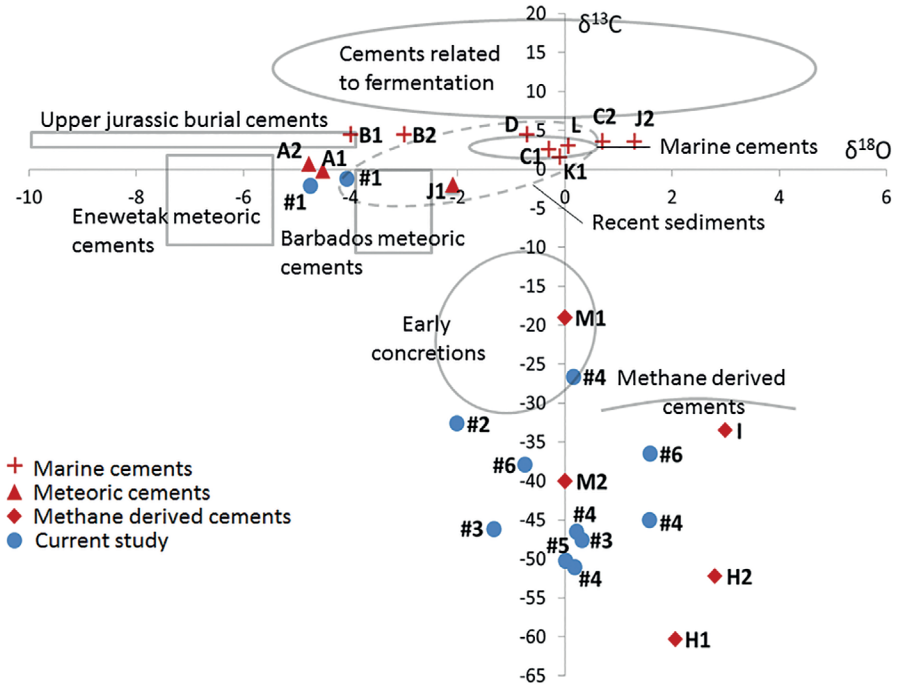

Figure 7. $\delta^{13}C$ versus $\delta^{18}O$ isotopic data from present work and A1, A2 - Spurgeon et al., 2003; B1, B2 - Calvet et al., 2003; C1, C2 - Webb et al., 1999; D - Beier, 1985; H1, H2 - Hovland et al., 1987; I - Lavoie et al., 2010; J1, J2 - Guerra et al., 2004; K1 - Barreto et al., 2010; L - Vieira and DeRos, 2007; M1, M2 - Roberts and Whelan, 1974 (Absent $\delta^{18}O$ data).

on Siesta Key, Florida. $\delta^{18}O$ isotopic values of sample 1 are a good indicator that it would have formed under freshwater conditions or influence, whilst remaining samples would have been formed in a mixed marine/freshwater environment.

Cements mineralogy and diagenetic features

Accordingly to Folk (1974) carbonate cements patterns and mineralogy are controlled by crystallization and Mg/Ca rates present on the fluid from which they precipitate, thus being an indicator of its formation environment. Magnesium controls the lateral growth of calcite, therefore, in Mg-rich environment such as shallow marine, calcium carbonate precipitates mainly as acicular aragonite and rhombic microcrystalline high-Mg calcite. In meteoric environments low magnesium rates lead to spar calcite and euhedral low-Mg calcite (Given and Wilkinson, 1985).

On sample 1, cements found were exclusively composed by microcrystalline, blocky druse and acute scalenohedral calcite crystals, the latter being interpreted as "dogtooth" (Flugel, 2010) or bladed (Scholle and Ulmer-Scholle, 2003) cements. Such cements would be indicators of formation in a near-surface active meteoric environment and such formation environment is corroborated by its isotopic values. Precipitation rates are lower due to lower ionic concentration and CO_2 degassing (Longman, 1980; Flugel, 2010), resulting in spar crystals observed in this sample (Folk, 1974). Microcrystalline cements are indicators of rapid precipitation during initial cementation process. Neomorphism of older cement has not been observed, but the partial dissolution of some bioclasts and its filling by blocky and microcrystalline cements may indicate that the main origin for the calcium carbonate is from the dissolution of bioclasts through fresh and vadose water fluxes. Bryozoan skeletons are usually composed of low-Mg calcite (Scholle and Ulmer-Scholle, 2003).

LMC circumgranular and granular mosaics on sample 6 are also indicative of a meteoric-phreatic, meteoric-vadose influence or shallow burial precipitation (Folk, 1974; Longman, 1980). These cements when observed on SEM have a "framboidal" characteristic, resulting

from rhombic crystals overlapping laterally. Similar results have been observed by Garrison et al. (1969).

Samples 2, 3, 4 and 5 all presented microcrystalline HMC coatings and cuticles around framework grains, preceding other diagenetic features on an initial cementation process, sometimes completely filling intergranular spaces. Acicular and fibrous aragonite and fibrous HMC have been abundantly observed on these samples. Such cement types are correlated to phreatic marine environments in all observed features, such as pore filling and pore lining spar, prismatic fringes, splays and botryoids. These cements develop preferably on Mg-rich environments such as shallow marine, and the length and lathlike development of the crystals is an indicative high CO^{3-} availability, thus a high energy environment (Folk, 1974; Given and Wilkinson, 1985).

Granular mosaics and circumgranular cements (Flugel, 2010) observed on incorporated fragments of sample 4 could have been either formed on a burial environment or on a marine-vadose environment. Infiltrated micrite, rich in fossils and siliciclastic silt-sized grains, are very likely the result of a later exposure on the continental shelf.

CONCLUSIONS

Based on isotopic and diagenetic characteristics of studied sandstones there is no evidence that these might have been formed on an "intertidal zone of an exposed beach" and therefore these cannot be considered as true beachrocks according to Hopley (1986).

It is possible to infer that sample 6 was formed under freshwater influence, most probably on an active meteoric environment. It is certain that this sedimentary deposit has remained exposed for at least 15.000 years before sea-level has reached its current position after the LGM. Cements possibly originated from the dissolution of the shells within this deposit, as small dissolution and recrystallization could be observed on some of the bioclasts. Calcite, the most stable form of carbonate (Vousdoukas et al., 2007), has remained bonding sediments together even after transgressive events. There is no clear evidence that this sample is from a true beachrock and this sandstone is likely to represent paleo phreatic-level, where exact sea-level cannot be inferred from collected and analyzed data.

Ages of samples collected on the inner-shelf at depths of 29 m (2) and 18 m (5) have ranged between 7913 and 7452 calibrated years BP. The distance between these two samples is 15 km perpendicular to the actual coastline orientation. Their isotopic composition suggests that cement precipitation on these sandstones has been promoted by methane migration through the sedimentary column. Cementation would have occurred in two possible ways:

Initially on a shallow burial environment with a limited circulation of water between pore spaces, when HMC crypto to microcrystalline cements resulted in an incipient to well-developed cementation (e.g. Longman, 1980) in a linked organic-matter rich environment such as deltas or marshes. After this initial cementation transgression would have exposed lithified material on an active marine phreatic environment. This allowed extensive growth of fibrous and acicular marine cements composed of HMC and aragonite, completely filling intergranular spaces and forming tight meshes and polygonal contacts, a typical characteristic of such formation environment.

b) After the transgression and drowning of Pleistocene organic-rich deposits when methane migrating through sedimentary column has prompted initial cementation on subsurface. Then later exposure to the water-sediment boundary and finally to an active marine phreatic environment would also have led to the same cement fabrics as described above. In this case, rather than ages being the result of a complex connected environment, they would reflect the ages of organic matter rich deposits that existed prior to last sea-level maximum and their formation would have no temporal correlation.

Incorporated fragments found on 21 m depth sample (4) could suggest that the first possibility is more likely to be plausible, but even in such depths currents can transport and rework material. Both suggestions could explain why samples more than 15 km apart from each other have yielded similar ages.

Relying on hand samples, the lack of lateral continuity and impossibility of observing structures *in situ* can pose a problem when trying to identify origin and history of complex lithified material in a dynamic environment. Through petrographic, geochemical and isotopic analysis it was possible to determine that these structures may have distinct diagenetic processes than beachrocks and that further analysis and observations are necessary in order to consider its use as a paleo-sea level indicator.

ACKNOWLEDGMENTS

BIS and LHSO were both supported by CAPES scholarship. RJA and MCS are sponsored by CNPq fellowships (303940/2014-0, 305691/2014-7). RJA is also sponsored by Fundação Araucária senior fellowship (45725).

The authors would like to thank Dr. Alcides Nobrega Sial for providing isotopic analysis performed at the NEG-LABISE from Universidade Federal de Pernambuco; Dr. Marcela Marques Vieira (UFRN) for corrections and discussions throughout the project; Dr. Luiz Alberto Fernandes (UFPR) for assistance on microscopic analysis; Universidade Federal do Paraná for infrastructure and laboratorial analysis (LAMIR, LabESed, CME).

Funding: This work was supported by Fundação Araucária (Protocolo 451 project) 001/2000 call and CAPES scholarships.

REFERENCES

ADAMS, A. E. & MACKENZIE, W. S. 1998. *A colour atlas of carbonate sediments and rocks under the microscope*, London, Manson Publishing.

ALLIOTA, S. SPAGNUOLO, J. O. & FARINATI, E. A. 2009. Origen de una roca de playa en la región costera de Bahía Blanca, Argentina. *Pesquisas em Geociências*, 36, 107-116.

ANGULO, R. J. 1993. Variações na configuração da linha de costa no Paraná nas últimas quatro décadas. *Boletim Paranaense de Geociências*, 41, 52-72.

ANGULO, R. J. 1999. Caracterização morfológica dos deltas de maré do litoral do estado do Paraná. *Anais da Academia Brasileira de Ciências*, 71, 935-959.

ANGULO, R. J. 2004. Mapa do Cenozóico do estado do Paraná. *Boletim Paranaense de Geociências*, 55, 25-42.

ANGULO, R. J., SOUZA, M. C., REIMER, P. J. & SASAOKA, S. K., 2005. Reservoir effect of the Southern and southeastern Brazilian coast. *Radiocarbon*, 47, 67-73.

ANGULO, R. J., LESSA, G. C. & SOUZA, M. C. 2006. A critical review of mid- to late-Holocene sea-level fluctuations on the eastern Brazilian coastline. *Quaternary Science Reviews*, 25, 486-506.

ANGULO, R. J., SOUZA, M. C., ASSINE, M. L., PESSENDA, L. C. R. & DISARÓ, S. T. 2008. Chronostratigraphy and radiocarbon age inversion in the Holocene regressive barrier of Paraná, Southern Brazil. *Marine Geology*, 252, 111-119.

ANGULO, R. J. & SOUZA, M. C. 2014. Conceptual review of Quaternary coastal paleo-sea level indicators from Brazilian coast. *Quaternary and Environmental Geosciences*, 5, 1-32.

BAHR, A., PAPE, T., BOHRMANN, G., MAZZINI, A., HAECKEL, M., REITZ, A. & 500 IVANOV, M. 2007. Authigenic carbonate precipitates from the NE Black Sea: a mineralogical, geochemical, and lipid biomarker study. *International Journal of Earth Sciences*, 98, 677-695.

BARRETO, A. M. F., ASSIS, H. M. B., BEZERRA, F. H. R. & SUGUIO, K. 2010. Arrecifes, a Calçada do Mar de Recife, PE - Importante registro holocênico de nível relativo do mar acima do atual. In: WINGE, M., SCHOBBENHAUS, C., SOUZA, C. R. G., FERNANDES, A. C. S., BERBERT-BORN, M. & SALLUN-FILHO, W., QUEIROZ, E. T. (eds.) *Sítios Geológicos e Paleontológicos do Brasil. Brasília*, DF: CPRM.

BEIER, J. A. 1985. Diagenesis of Quaternary Bahamian beachrock: petrographic and isotopic evidence. *Journal of Sedimentary Petrology*, 55, 755-761.

BENITES, M., ALVES, D., MALY, M. & JOVANE, L. 2015. Shallow gas occurrence in a Brazilian (Saco do Mamanguá, Rio de Janeiro) inferred from high-resolution seismic data. *Continental Shelf Research*, 108, 89-96.

BIGARELLA, J. J. 2001. Contribuição ao estudo da Planície Litorânea do estado do Paraná. *Brazilian Archives of Biology and Technology, Jubilee*, 65-110.

BRANNER, J. C. 1904. The stone reefs of Brazil, their geological and geographical relations, with a chapter on the coral reefs. *Bulletin of the Museum of Comparative Zoology at Harvard College 44*, Geological Series 7. Cambridge, MA, Harvard College.

BURDIGE, D. J. 2006. *Geochemistry of marine sediments*, New Jersey, Princeton University Press.

CABRAL NETO, I., CÓRDOBA, V. C. & VITAL, H. 2010. Petrografia de beachrock em zona costa afora adjacente ao litoral norte do Rio Grande do Norte, Brasil. *Quaternary and Environmental Geosciences*, 2, 12-18.

CALLIARI, L. J., ESTEVES, L. S., OLIVEIRA, C. P. L., TOZZI, H. A. M., SILVA, R. P. & CARDOSO, J. N. 1994. Padrões sonográficos e sedimentológicos de um afloramento de beachrock na plataforma interna do Rio Grande do Sul (COMEMIR/OSNLR). *Notas Técnicas*, 7, 27-32.

CALVET, F., CABRERA, M. C., CARRACEDO, J. C., MANGAS, J., PÉREZ-TORRADO, F. J., RECIO, C. & TRAVÉ, A. 2003. Beachrocks from the island of La Palma (Canary Islands, Spain). *Marine Geology*, 197, 75-93.

CHAVES, N. & SIAL, A. 1998. Mixed oceanic and freshwater depositional conditions for beachrocks of northeast Brazil: Evidence from carbon and oxygen Isotopes. *International Geology Review*, 40, 748-754.

CHOQUETTE, P. W. & TRUSELL, F. C. 1978. A procedure for making the titan-yellow stain for Mg-calcite permanent. *Journal of Sedimentary Research*, 48, 639-641.

DELANEY, J. 1965. Reef rock on the coastal platform of southern Brazil and Uruguay. *Symposium on the ocean of western South Atlantic - Brazil*, Sect. III, 9.

EMERY, K. O. & COX, D. C. 1956. Beachrock in the Hawaiian Islands. *Pacific Science*, 10, 382-402.

FELIX, C. A. & MAHIQUES, M. M. 2013. *Late quaternary evolution and shallow gas formation in a tropical estuarine environment: the case of the Bertioga channel, Brazil. 2013 IEEE/OES Acoustics in Underwater Geosciences Symposium*. Jul 24-26; Rio de Janeiro, RJ, Brazil.

FLUGEL, E. 2010. *Microfacies of Carbonate Rocks: Analysis, Interpretation and Application*, Berlin, Springer-Verlag.

FRIEDMAN, G. M., SANDERS, J. E., ELIEZER, G. & ALLEN, R. C. 1971. Marine lithification mechanism yields rock resembling beachrock. *In*: BRICKER, O. P. (ed.) *Carbonate Cements*. Baltimore: Johns Hopkins Press.

FOLK, R. L. 1974. The natural history of crystalline calcium carbonate: effect of magnesium content and salinity. *Journal of Sedimentary Petrology*, 44, 40-53.

FÚLFARO, V. J. & AMARAL, G. 1970. Trend surface analysis das areias da praia do Tenório, Ubatuba, SP. *XXIV Congresso Brasileiro de Geologia; Brasília*, 299-305.

GISCHLER, E. & LOMANDO, A. J. 1997. Holocene cemented beach deposits in Belize. *Sedimentary Geology*, 110, 277-297.

GIVEN, K. R. & WILKINSON, B. H. 1985. Kinetic control of morphology, composition and mineralogy of abiotic sedimentary carbonates. *Journal of Sedimentary Petrology*, 55, 109-119.

GUERRA, N. C. & SIAL, A. N., 2003. Diagenetic model for beachrocks of the Alagoas State, Northeastern Brazil: isotopic and petrographic evidence. *IV South American Symposium on Isotope Geology Short Papers; Salvador*, *BA, Brazil*. 357-358.

GUERRA, N. C., KIANG, C. H. & SIAL, A. N., 2004. Carbonate cements in contemporaneous beachrocks, Jaguaribe beach, Itamaracá Island, northeastern Brazil: petrographic, geochemical and isotopic aspects. *Anais da Academia Brasileira de Ciências*,77, 343-352.

HAN, X., SUESS, E., HUANG, Y., WU, N., BOHRMANN, G., SU, X., EISENHAUER, A., REHDER, G. & FANG, Y. 2008. Jiulong methane reef: Microbial ediation of seep carbonates in the South China Sea. *Marine Geology*, 249, 243-256.

HOPLEY, D. 1986. Beachrock as a sea-level indicator. In: VAN DER PLASCHE, O. (ed.) *Sea-level Research: a manual for the collection and evaluation of data*. Norwich: GeoBooks.

HOVLAND, M., TALBOT, M. R., QVALE, H., OLAUSSEN, S. & AASBERG, L. 1987. Methane-related carbonate cement in pockmarks of the North Sea. *Journal of Sedimentary Petrology*, 57, 881-892.

JUDD, A. G. & HOVLAND, M. 1992. The evidence of shallow gas in marine sediments. *Continental Shelf Research*, 12, 1081-1095.

KELLETAT, D. 2006. Beachrock as sea-level indicator? Remarks from a geomorphological point of view. *Journal of Coastal Research*, 22, 1555-1564. KELLETAT, D. 2007. Reply to: KNIGHT, J. 2007. Beachrock Reconsidered.

Discussion of: KELLETAT, D., 2006. Beachrock as Sea-Level Indicator? Remarks from a Geomorphological Point of View, Journal of Coastal Research, 22, 1558-1564; Journal of Coastal Research, 23, 1074-1078. *Journal of Coastal Research*, 23,1605-1606.

KINDLER, P. & BAIN, R. J. 1993. Submerged upper Holocene beachrock on San Salvador Island, Bahamas: implications for recent sea-level history. *Geologische Rundschau*, 82, 241-247.

KLEIN, A. H. F., DEMARCO, L. F. W., GUESSER, V., FLEMMING, G. R., BONETTI, J., PORPILHO, D., AYRES NETO, A., SOUZA, J. A. G. & FÉLIX, C. A. 2016. Shallow gas seismic structures: forms and distribution on Santa Catarina Island, Southern Brazil. Brazilian Journal of Oceanography, 64, 325-338.

KNIGHT, J. 2007. Beachrock Reconsidered. Discussion of: KELLETAT, D., 2006. Beachrock as Sea-Level Indicator? Remarks from a Geomorphological Point of View, *Journal of Coastal Research*, 22, 1558-1564. Journal of Coastal Research, 23, 1074-1078.

LAVOIE, D., PINET, N., DUCHESNE, M., BOLDUC, A. & LAROCQUE, R. 2010. Methane-derived authigenic carbonates from active hydrocarbon seeps of the St. Lawrence Estuary, Canada. *Marine and Petroleum Geology*, 27, 1262-1272.

LONGMAN, M. W. 1980. Carbonate diagenetic textures from nearsurface diagenetic environments. *The American Association of Petroleum Geologists Bulletin*, 64, 461-487.

MANSUR, K. L., RAMOS, R. R. C., GODOY, J. M. & NASCIMENTO, V. M. R. 2011. Beachrock de Jaconé, Maricá e Saquarema - RJ: importância para a história da ciência e para o conhecimento geológico. *Revista Brasileira de Geociências*, 41, 290-303.

MANSO, V. A. V., CORRÊA, I. C. S. & GUERRA, N. C. 2003. Morfologia e Sedimentologia da Plataforma Continental Interna entre as Praias Porto de Galinhas e Campos - Litoral Sul de Pernambuco, Brasil. *Pesquisas em Geociências*, 30, 17-25.

MARTINS, L. R., URIEN, C. M. & MARTINS, I. R. 2005. Gênese dos sedimentos da Plataforma Continental Atlântica entre o Rio Grande do Sul (Brasil) e Tierra del Fuego (Argentina). *Gravel*, 85-102.

MILLIMAN, J. D. & EMERY, K. O. 1968. Sea levels during the Past 35,000 Years. 601 *Science*, 162, 1121-1123.

MORAIS, J. O., IRION, G. F., PINHEIRO, L. S. & KAHSBOM, J. 2009. Preliminary results on Holocene sea-level changes on Cerá Coast/ Brazil. *Journal of Coastal Research*, 603 56, 646-649.

MOORE, C. H. 1989. *Carbonate diagenesis and porosity*. Amsterdam, Elsevier.

MUEHE, D. & CARVALHO, V. G. 1993. Geomorfologia, cobertura sedimentar e transporte de sedimentos na plataforma continental interna entre a Ponta de Saquarema e o 607 Cabo Frio (RJ). *Boletim do Instituto Oceanográfico*, 41, 1-12.

NELSON, C. S. & LAWRENCE, M. F. 1984. Methane-derived high-Mg calcite submarine cements in Holocene nodules from the Fraser Delta, British Columbia, Canada. *Sedimentology*, 31, 645-654.

PETTIJOHN, F. J., POTTER P. E. & SIEVER, R. 1987. *Sand and Sandstone*. New York, Springer-Verlag.

REIMER, P. J., BAILLIE, M. G. L., BARD, E., BAYLISS, A, BECK, J. W., BLACKWELL, P. G., BRONK RAMSEY, C., BUCK, C. E., BURR, G. S., EDWARDS, R. L., FRIEDRICH, M., GROOTES, P. M., GUILDERSON, T. P., HAJDAS, I., HEATON, T. J., HOGG, A. G., HUGHEN, K. A., KAISER, K. F., KROMER, B., MCCORMAC, F. G., MANNING, S. W., REIMER, R. W., RICHARDS, D. A., SOUTHON, J. R., TALAMO, S., TURNEY, C. S. M., VAN DER PLICHT, J. & WEYHENMEYER, C. E. 2009. IntCal09 and Marine09 radiocarbon age calibration curves, 0–50,000 years cal BP. *Radiocarbon*, 51, 1111-1150.

REY, D., RUBIO, B., BERNABE, A. M. & VILAS, F. 2004. Formation, exposure and evolution of a high-latitude beachrock in the intertidal zone of the Corrubedo complex (Ria de Arousa, Galicia, NW Spain). *Sedimentary Geology*, 169, 93-105.

ROBERTS, H. H. & WHELAN, T. 1975. Methane-derived carbonate cements in barrier and beach sands of a subtropical delta complex. *Geochimica et Cosmochimica Acta*, 39, 1085-1089.

RUSSELL, R. J. & MCINTIRE, W. G. 1965. Southern hemisphere beach rock. *Geographical Review*, 55, 17-45.

SIESSER, W. G. 1974. Relict and recent beachrock from southern Africa. *Geological Society of America Bulletin*, 85, 1849-1854.

SCHOLLE, P. A. & ULMER-SCHOLLE, D. S. 2003. A color guide to the petrography of carbonate rocks: grains, textures, porosity, diagenesis. Volume 77. Tulsa, American Association of Petroleum Geologists.

SCHROEDER, J. H. 1979. Carbonate diagenesis in Quaternary beachrock of Uyombo, Kenya: sequences of processes and coexistence of heterogenic products. *Geologische Rundschau*, 68, 894-919.

STOW, D. A. V. 2005. *Sedimentary Rocks in the Field: A Colour Guide*, London: Manson Publishing.

STUIVER, M., REIMER. P. J. & REIMER, R.W. 2009. CALIB 6.0. Internet Program and Documentation [cited 2017 Dec 5]. Available from: http://calib.org/calib/

SUGUIO, K., RODRIGUES, S. A., TESSLER, M. G. & LAMBOOY, E. E. 1984. Tubos de Ophiomorphas e outras feições de bioturbação na Formação Cananéia, Pleistoceno da planície costeira Cananéia-Iguape, SP. In: *III Simpósio Regional de Geologia, Niterói, RJ*. Restingas: origem, estrutura, processos, 111-122.

SUGUIO, K., MARTIN, L., BITTENCOURT, A. C. S. P., DOMINGUEZ, J. M. L., FLEXOR, J. M. & AZEVEDO, A. E. G. 1985. Flutuações do nível relativo do mar durante o Quaternário superior ao longo do litoral brasileiro e suas implicações na sedimentação costeira. *Revista Brasileira de Geociências*, 15, 273-286.

SPURGEON, D., DAVIS, J. R. A. & SHINN, E. A. 2003. Formation of 'Beach Rock' at Siesta Key, Florida and its influence on barrier island development. *Marine Geology*, 200, 19-29.

VANHONI, F. & MENDONÇA, F. 2008. O clima do litoral do estado do Paraná. *Revista Brasileira de Climatologia*, 3, 50-63.

VEIGA, F. A., ANGULO, R. J., MARONE, E. & BRANDINI, F. P. 2004. Características sedimentológicas da plataforma interna rasa na porção central do litoral *Paranaense. Boletim Paranaense de Geociências*, 55, 67-75.

VEIGA, F. A., ANGULO, R. J., SÁ, F., ODRESKI, L. L. R., LAMOUR, M. R. & DISARÓ, S. T. 2006. Origin of mud deposits in a wave dominated shallow inner continental shelf of the State of Paraná coast, southern Brazil. *Journal of Coastal Research*,39, 262-265.

VIEIRA, M. M., DEROS, L. F. & BEZERRA, F. H. R. 2006. Lithofaciology and Palaeoenvironmental Analysis of Holocene Beachrocks in Northeastern Brazil. *Journal of Coastal Research*, 23, 1535-1548.

VIEIRA, M. M. & DEROS, L. F. 2007. Cementation patterns and genetic implications of Holocene beachrocks from northeastern Brazil. *Sedimentary Geology*, 192, 207-230.

VOUSDOUKAS, M. I., VELEGRAKIS, A. F. & PLOMARITIS, T. A. 2007. Beachrock occurrence, characteristics, formation mechanisms and impacts. *Earth-Science Review*, 85, 23-46.

VOUSDOUKAS, M. I., VELEGRAKIS, A. F. & KARAMBAS, T. V. 2009. Morphology and sedimentology of a microtidal beach with beachrocks: Vatera, Lesbos, NE Mediterranean. *Continental Shelf Research*, 29, 1937-1947.

WARNE, J. 1962. A quick field or laboratory staining scheme for the differentiation of the major carbonate minerals. *Journal of Sedimentary Petrology*, 32, 29-38.

WEBB, G. E., JELL, J. S. & BAKER, J. C. 1999. Cryptic intertidal microbialites in beachrock, Heron Island, Great Barrier Reef: implications for the origin of microcrystalline beachrock cement. *Sedimentary Geology*, 126, 317-334.